

# Evaluation of a high-speed hybrid OAM-OFDM-MDM multiplexed coherent FSO system under desert conditions

SHIVAJI SINHA, CHAKRESH KUMAR\*

University School of Information, Communication & Technology,  
Guru Gobind Singh Indraprastha University,  
Sector - 16 C, Dwarka, New Delhi - 110078, India

\*Corresponding author: ckumardhan@gmail.com

To meet the needs of future wireless optical networks, this paper introduces a high-speed, hybrid multiplexed, coherent free-space optical (FSO) communication system that integrates an orbital angular momentum (OAM) multiplexed signal with an orthogonal frequency division multiplexing (OFDM) technique. Two independent QAM polarized beams, each carrying in-phase and quadrature (I/Q) phase 16-QAM-OFDM modulated data, are combined using mode division multiplexing (MDM) to increase the capacity of the proposed system. The reason of choosing OFDM is its capability to support higher data rate, and mitigating intersymbol interference (ISI). The signal is detected using a coherent detection-based digital signal processing (DSP) algorithm at the receiver end. The proposed hybrid FSO system is evaluated in low and heavy dust environments using bit error rate (BER), link distance, optical signal-to-noise ratio (OSNR), and received optical power performance matrices. The simulation results demonstrate the successful transmission of a 120 Gb/s single carrier over the longest link ranges of 1.5 and 0.40 km, respectively, under low and heavy dust weather environments below the signal degradation threshold value (forward error correction (FEC) limit) of  $BER\ 2.2 \times 10^{-3}$  in strong turbulent conditions.

Keywords: atmospheric attenuation, bit error rate (BER), orbital angular momentum (OAM), optical signal-to-noise ratio (OSNR), orthogonal frequency division multiplexing (OFDM), quadrature amplitude modulation (QAM), transmission range.

## 1. Introduction

The increasing demand for cost-effective high-speed data streaming due to exponential growth in end users has been emerging as a big challenge for conventional radio frequency (RF) and microwave transmission networks due to a lack of infrastructure, last-mile challenges, and regulatory issues. Due to the growth of data traffic, it is estimated that the RF spectrum will be exhausted in the next few years. However, the use of the optical spectrum will have a significant potential to meet the constantly expanding demand for this data traffic. Free-space optical (FSO) communication, which offers very

huge data rates (in Gb/s) in the optical domain, has been found to be an alternative wireless technological solution that can overcome all of the above discussed challenges by providing quick infrastructure installation, abundant license-free bandwidth, and high-speed, secure data transmission [1-4].

The major challenges in optical signal transmission through the free space channel are the atmospheric attenuation due to molecular absorption, scattering, and the scintillation phenomenon, which highly degrade the transmission link. The performance of the high speed FSO link has been investigated under various atmospheric conditions such as heavy rain, smoke, snow, fog, and dust by the various research groups. Various solutions have been proposed to enhance the data rate of the FSO link in previously discussed weather conditions [5-9].

Recently, the work in [10] investigated the transmission of 10 Gb/s-60 GHz hybrid fiber/FSO link using orthogonal division multiplexing (OFDM) and incorporating doublet lens technique to enhance the transmission link and reduce the multipath fading and dispersion effect for 50 km fiber and 0.5 km FSO links with good BER for 16-QAM modulation. MUKHERJEE *et al.* presented a cost effective and secure 88 Gb/s FSO system over 0.550 km link using 4-PPM with self-injection locked-quantum dash laser diode (QD-LD) and Reed–Solomon (RS) channel encoding which help in decreasing the power penalty [11]. DUTTA *et al.* studied the hybrid orbital angular momentum and wavelength division multiplexing (OAM-WDM)-based FSO system to realize 100 Gb/s FSO links over 3.2 km under clear weather, haze, rain, and fog weather conditions. A very low BER of  $5 \times 10^{-9}$  and a good quality factor (Q) of 5.4 are obtained for a 2.4 dB power penalty [12]. A 640 Gb/s data transmission over 180 m link distance is demonstrated by multiplexing of 4 OAM modes in FSO system. A 640 Gb/s data transmission over a 180 m link distance is demonstrated by the multiplexing of four OAM modes in the FSO system. The remarkable results have been achieved with a very low 2.91 dB power penalty at a BER of less than  $10^{-9}$  and an excellent Q-factor more than 5.5 [13]. ABD EL-MOTTALEB *et al.* has reported the performance of the spectral amplitude coding-optical code division multiple access (SAC-OCDMA) system by employing enhanced double weight (EDW) signature codes and multiple access interference (MAI) techniques. The implementation of MAI in the proposed SAC-OCDMA system leads to degradation in system performance, which is further resolved by using a single photodiode detection technique (SPD). A comparison between the EDW and modified double weight (MDW) codes is also demonstrated in terms of BER, Q-factor, and received optical power [14]. Recently, the hybrid SAC-OCDMA-MDM FSO system has been investigated to increase the system capacity in which a 100 Gb/s data is transported over 8 km turbulent link by using two Laguerre–Gaussian (LG) modes and detected at the receiver by direct detection method [15]. SIVARAJANI *et al.* achieved an improvement in data rate of about 4 Gb/s with a power of 25 dBm in a FSO system considering an underground moving train environment for a maximum link range of 1.4 km using performance metrics of BER, OSNR, Q-factor, and received optical power [16]. Dense wavelength division multiplexing (DWDM) is a bandwidth efficient solution which increases the capacity of the FSO link. KUMAR *et al.* successfully

demonstrated the implementation of a  $5 \times 16$  Gb/s DWDM FSO system with a frequency spacing of 100 GHz under clear sky conditions for a link of 38 500 km. The results showed that with increasing transmitted optical power, the Q-factor also increases, while it decreases with increasing atmospheric turbulence effects [17].

Recently, many researchers have focused on the space division multiplexing (SDM) technique, in which the spatially distributed intensity pattern of the optical carrier signal is used to carry binary information using orbital angular momentum (OAM). The laser beam carrying a QAM signal possesses two distinct characteristics: inherent orthogonality and unbounded states in principle. These features are very useful to increase the FSO system bandwidth and the information carrying capacity by transmitting multiple information streams simultaneously using QAM multiplexing [18].

In this paper, a new high-speed and spectral-efficient hybrid FSO system has been proposed by incorporating the features of OAM optical beams carrying two Laguerre–Gaussian (LG) modes  $LG_{0,0}$  and  $LG_{0,13}$ , respectively. The main objective of this paper is to achieve a data rate of 120 Gb/s, by integrating the hybrid multiplexing (OAM, OFDM and MDM) techniques under different dust storms weather conditions with an intensity scintillation effect. The two OAM optical beams carry independent data stream simultaneously without any crosstalk whereas OFDM and the single carrier 16-QAM format help out to achieve high data rate with robust signal transmission. The system performance is investigated using BER, link distance, OSNR and eye diagram.

The rest of the paper is structured as follows: Section 2 illustrates the proposed model and describes the working principle of the transceiver system in detail. Sections 3 and 4 explain the mathematical analysis of the FSO channel and losses incurred due to strong storm conditions. Finally, the system performance is investigated using the simulation results in Section 5, followed by the conclusions drawn in Section 6.

## 2. Proposed schematic diagram and working principle

The design schematic of the proposed 16-QAM modulated OAM-OFDM-MDM free space optical link has been discussed in this section. The system comprises of optical transmitter system, atmospheric FSO channel and coherent homodyne receiver as illustrated in Fig. 1.

The optical transmitter section consists of a pseudorandom bit sequence (PRBS) generator used to generate binary information, which is then converted to a parallel binary stream for serial-to-parallel (S/P) block output. These parallel binary sequences are then encoded in non-return to zero binary signal in NRZ block and then converted to OFDM modulated signal. The output from this block is fed to the OAM polarized (OP) 16-QAM modulator system. The laser beam of continuous wave (CW) spatial laser splits into two independent OAM polarized beams,  $LG_{0,0}$  and  $LG_{0,13}$ , respectively. These two optical carriers further transport the in-phase and quadrature phase (I/Q) components of OP 16-QAM modulated signal. The OP 16-QAM modulator block composed of the M-ary pulse generator, lithium niobate Mach–Zehnder modulator

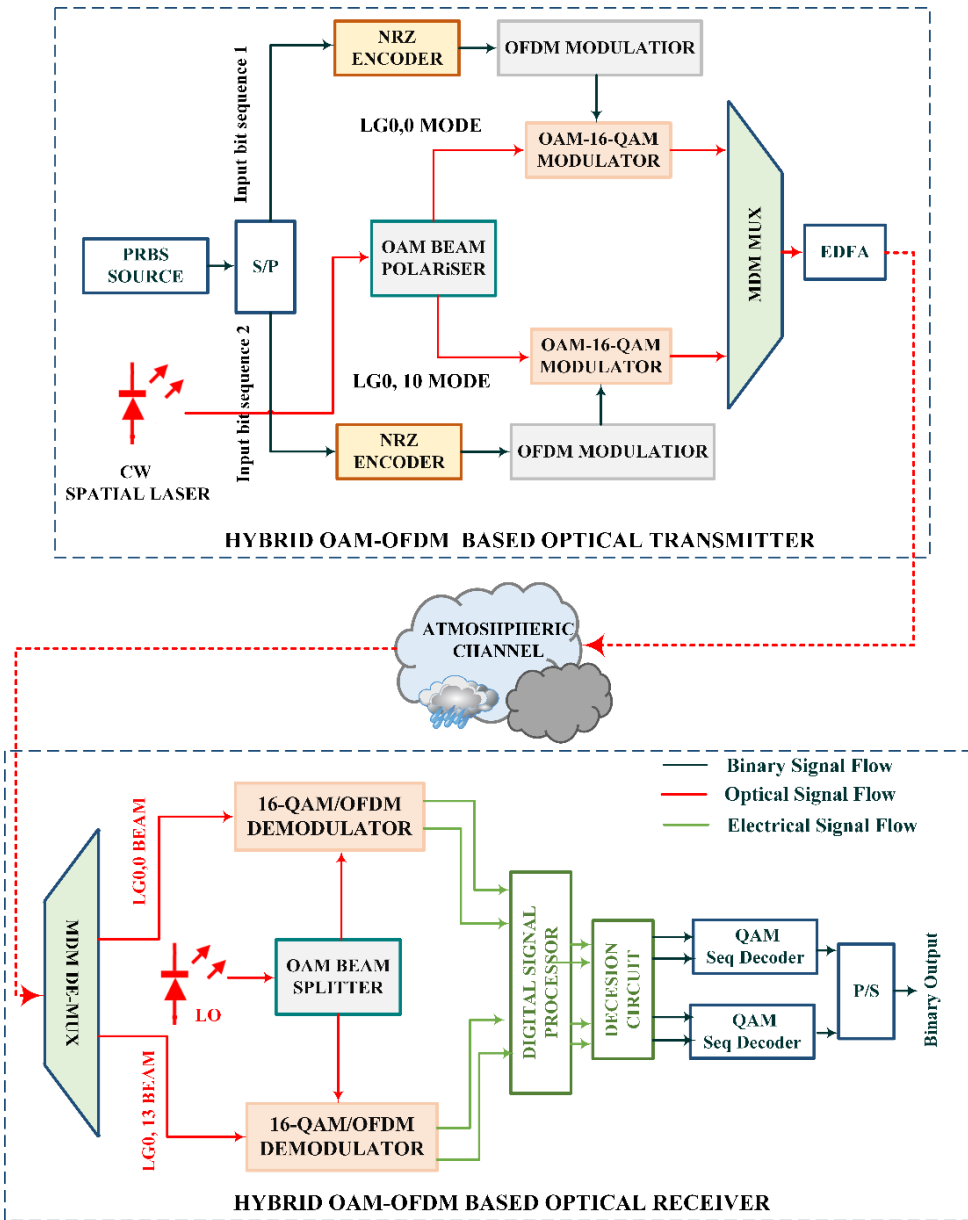


Fig. 1. Schematic and simulation setup demonstrating the OAM-OFDM-MDM FSO system.

(LiNbO<sub>3</sub>-MZM), dual-drive PRBS source and 90° phase-shifter as presented in Fig. 2. The relative phase difference in both the upper and lower arms is adjusted to 90°. The cross-coupler output consists of optically modulated 16-QAM signal with a bias of 4 V and -4 V. The sequence generator maps the incoming binary data into 4 bit 16-QAM symbols. In OFDM block, 12 training symbols and 8 pilot sub-carriers are

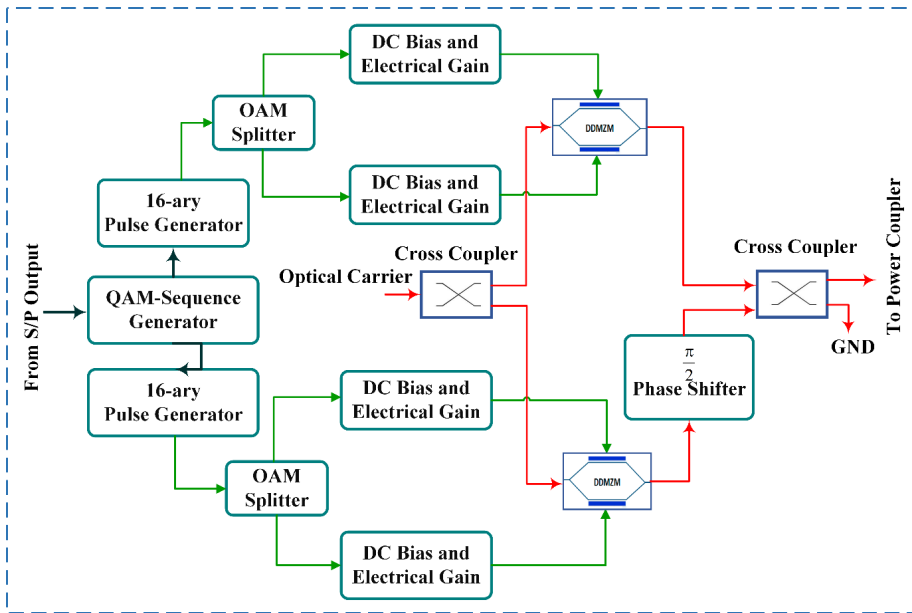


Fig. 2. Structure of OAM polarized internal 16-QAM optical modulator.

adopted for the carrier phase estimation (CPE) and FSO channel estimation. The power coupler (MDM) block combines these two OP 16-QAM signals, and the output is amplified in erbium-doped fiber amplifier (EDFA) to compensate for the attenuation provided by the turbulent free space channel and finally transmits over the turbulent channel under strong storm weather conditions.

At the receiver end, the received optical modes are isolated and fed to the upper and lower sections of the OAM polarized coherent homodyne receiver, respectively. The front-end section of the demodulator section shown in Fig. 3 performs different

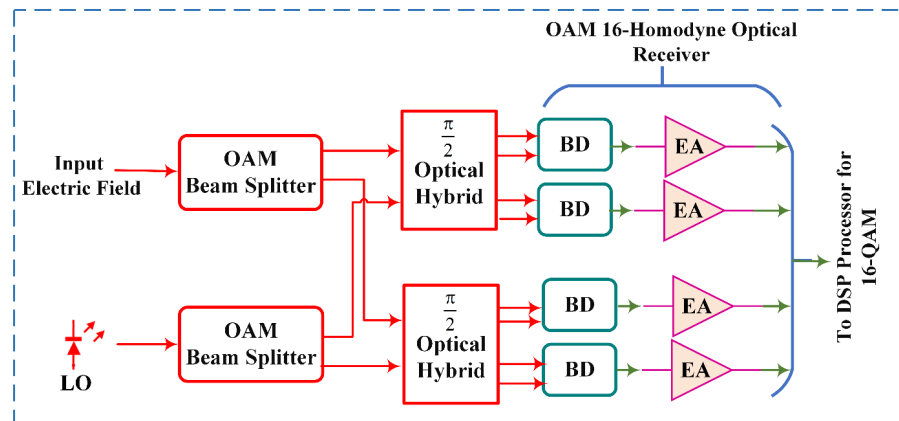


Fig. 3. Structure of OAM polarized 16-QAM homodyne optical receiver.

operations such as A/D conversion, dispersion compensation, cyclic prefix removal, channel estimation, and CPE. The balanced photo-detectors (BD), 90° optical hybrid, electronic amplifiers (EA), and a decision block are the major components of the coherent homodyne detector as shown in Fig. 3. Balanced photo-detector unit is used to minimize the intensity noise fluctuations in two branches by the subtraction of the photo-detector currents. The digital signal processing (DSP) block comprises of down sampling, equalizer, resampling and Bessel filter unit. The blind phase search (BPS) algorithm is implemented in DSP unit to minimize the phase difference between the optical transmitter and receiver [19,20]. The optical intensity variation in the lower and upper branches are cancelled out by the balanced photo-detectors. This next homodyne section recovers the M-ary pulses for both OAM optical modes and detects the transmitted binary information.

The modal analysis of the QAM optical beam, the mathematics of the turbulent FSO channel, and the different dust storm levels are discussed in the next section.

### 3. Modal analysis of OAM beam (Laguerre–Gaussian mode)

The helical phase front structure of an OAM optical beam is expressed by  $\exp(jn\theta)$ , where  $n$  is any integral value of  $2\pi$  phase shifts in the beam phase profile and  $\theta$  is the azimuthal angle, respectively. These beams can form an infinite number of orthogonal states when they propagate in a free space channel. Figure 4, shows the donut shaped

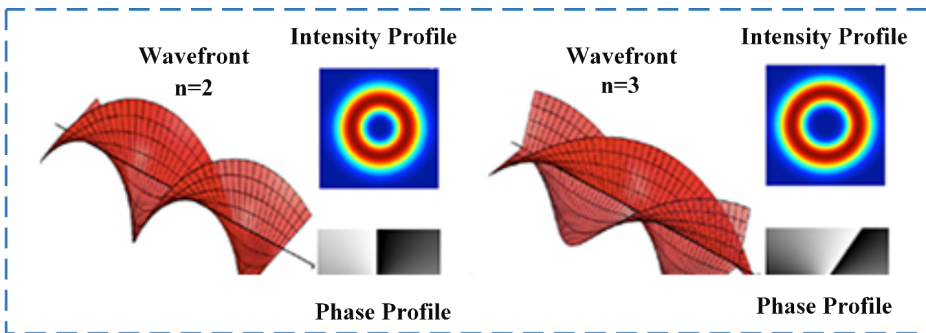


Fig. 4. Intensity and phase structure of donut shape OAM beams.

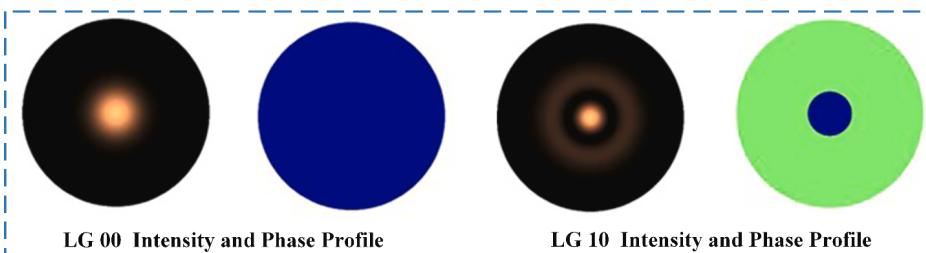


Fig. 5. Intensity and phase structure of Laguerre–Gaussian (LG<sub>00</sub> and LG<sub>10</sub>) OAM beam.

intensity and phase profile of the OAM beam for two states ( $n = 2$  and  $n = 3$ ), respectively. Whereas Fig. 5 illustrates the 2-D intensity and phase profile of the Laguerre–Gaussian beams carrying OAM signals considered for our proposed system.

The electric field of the LG, OAM beam can be represented mathematically in cylindrical coordinate as

$$\begin{aligned}
 E(r, \theta, z, n, p) = & \sqrt{\frac{2p!}{\pi(p + |n|)!}} \frac{1}{\omega(z)} \left[ \frac{r\sqrt{2}}{\omega(z)} \right]^{|n|} L_{p,n} \left[ \frac{2r^2}{\omega^2(z)} \right] \\
 & \times \exp \left[ \frac{-r^2}{\omega^2(z)} - \frac{jr^2 cz}{2(z^2 + z_R^2)} \right] \exp \left[ j(2p + |m| + 1) \tan^{-1} \frac{z}{z_R} \right] \exp(-jn\theta)
 \end{aligned} \tag{1}$$

where  $r$ ,  $\theta$  and  $z$  represent radial coordinates, angular coordinates, and beam propagation direction, respectively, and  $\omega(z)$  and  $z_R$  represent beam waist size and Rayleigh range, respectively. Here  $p = 0$  or  $1$  and  $n = 0$  are the modal indices in the  $r$  and  $\theta$  directions for LG ( $L_{p,n}$ ) polynomial, respectively chosen to increase the capacity of the proposed system using MDM. The reason of choosing only two lower order modes is the complexity in OAM multiplexing and de-multiplexing and the higher amount of intermodal crosstalk. The wave number is shown by  $c$ .

#### 4. Sand/dust storm characteristics and optical link attenuation

The channel characteristics of the FSO channel are dynamic with respect to time, and deteriorates the optical link performance under different weather conditions such as rain, haze, fog, storm, *etc.* These conditions can produce atmospheric attenuation, expressed by Eq. (2). The strength of this attenuation is determined by the cross-sectional dimensions, particle density in the channel, and transmitting wavelength.

$$L_{\text{atm}}(\text{dB/km}) = 10 \log \left( \frac{1}{T_a} \right) \tag{2}$$

where  $T_a$  shows the atmospheric transmittance. Whereas the largest free space path loss is expressed by

$$L_{\text{FS}}(\text{dB/km}) = \left( \frac{\lambda}{4\pi R} \right)^{-q} \tag{3}$$

Sand and dust storms are hard weather meteorological conditions that will interfere with the wireless optical link. They are caused by high wind velocity, which pulls ground dust particles from the ground into free space. These dust storms are classified as “light dust (LD)” and “heavy or moderate, and severe dust (SD)”, respectively [21].

T a b l e 1. Visibility and attenuation for different type of dust [22].

Dust type	LD	MD	SD
Visibility [km]	1–10	0.2–1	<0.2
Attenuation [dB/km]	25.11	107.66	297.38

Table 1 presents the visibility and the attenuation levels for different classes of dust storms. These dust storms are responsible for link degradation during the light beam transmission through the FSO channel. This dust attenuation depends on the link distance  $R$ , which can be given by

$$L_{\text{dust}}(\text{dB/km}) = 52 \times R^{-1.05} \quad (4)$$

The irradiance intensity due to the scintillation phenomenon within the cross-section of the detector plane is respectively defined in terms of scintillation index  $\sigma_I^2$  [23] and the received optical power at the receiver end [24] by the following equations:

$$\sigma_I^2 = \frac{\langle I^2 \rangle - \langle I \rangle^2}{\langle I \rangle^2} \quad (5)$$

$$P_t = 10^{-\alpha R/10} P_r \left( \frac{D_R^2}{D_T + \varphi R} \right) \quad (6)$$

where, the transmitter and receiver aperture diameters are  $D_T$  (m) and  $D_R$ , respectively, and  $R$  is transmission link range (km). Here,  $\varphi$  (mrad) represents the divergence angle, and  $\alpha$  is the attenuation coefficient in dB/km.

The Gamma-Gamma probability distribution function, which expresses the probability of the given optical intensity at the receiver end, is used to model atmospheric fading and given by

$$P(I) = \frac{2(\alpha\beta)^{\frac{\alpha+\beta}{2}}}{\Gamma(\alpha)\Gamma(\beta)} I^{\frac{\alpha+\beta}{2}-1} K_{\alpha-\beta}(2\sqrt{\alpha\beta I}) \quad (7)$$

where  $\alpha$  and  $\beta$  represent the small-scale and large-scale turbulence parameters, respectively, and  $K(\cdot)$  is the modified Bessel function of the second kind [25].

## 5. Simulation results and discussion

The proposed system performance is elucidated in this section and tested in terms of performance metrics BER with respect to different link distances, OSNR, and received optical power. The proposed system is evaluated under light and heavy sand or dust storm conditions assuming a fixed strong air turbulence scenario ( $5 \times 10^{-13} \text{ m}^{-2/3}$ ) to understand the degradation of the BER and to maximize the system capacity. The signal



T a b l e 2. System simulation parameters for the proposed link.

System parameters	Values
Spatial laser power	20 dBm
Bit rate	120 Gb/s
Baud rate	15 Gb/s
Sequence length	65536
Laser wavelength	1550 nm
Tx/Rx laser linewidth	0.01 MHz
Tx/Rx aperture diameter	10 cm
Beam divergence	0.20 mrad
Optical receivers losses	0 dB
Refractive index structure	$5 \times 10^{-13} \text{ m}^{-2/3}$
PD responsivity	1 A/W
Detector dark current	10 nA
Thermal noise power density	$10^{-22} \text{ W/Hz}$

attenuation due to large-size objects like trees, sign boards, buildings, geometric and misalignment losses and other weather conditions such as fog, rain, *etc.*, is assumed to be ideal during the simulation process. The PRBS block generates a sequence length of  $2^{17} - 1$  with random seed generation at the transmitter end whereas, the spatial laser produces a 20 dBm optical power at a wavelength of 1550 nm. The simulation parameters chosen for the proposed system are described in Tables 1 and 2, respectively. Both the  $\text{LiNbO}_3$  MZM modulators are fixed at extinction ratio of 25 dB at the null point of operation.

A discrete time delay is also introduced to model propagation delay, and the channel fading is assumed to be constant for the coherence time of  $5.22 \times 10^{-6} \text{ s}$  and changes

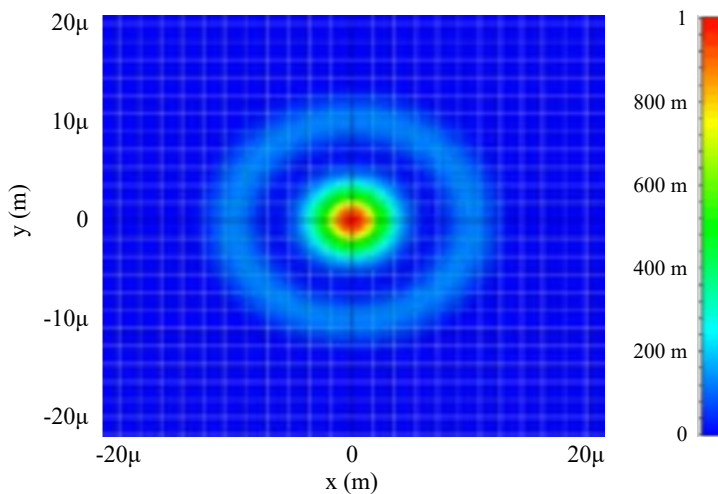


Fig. 6. Spatial intensity profile of MDM multiplexed OAM beam.

from one frame symbol to another frame for the proposed system. A user defined OSNR FEC limit is also set in each simulation graph to evaluate the link performance. Figure 6, shows the simulated spatial intensity profile of the transmitted MDM multiplexed OAM beams used in the proposed FSO system.

The BER performance is illustrated for different links as shown in Figs. 7–10 under different dust conditions for our proposed model system. On comparing the results, it is

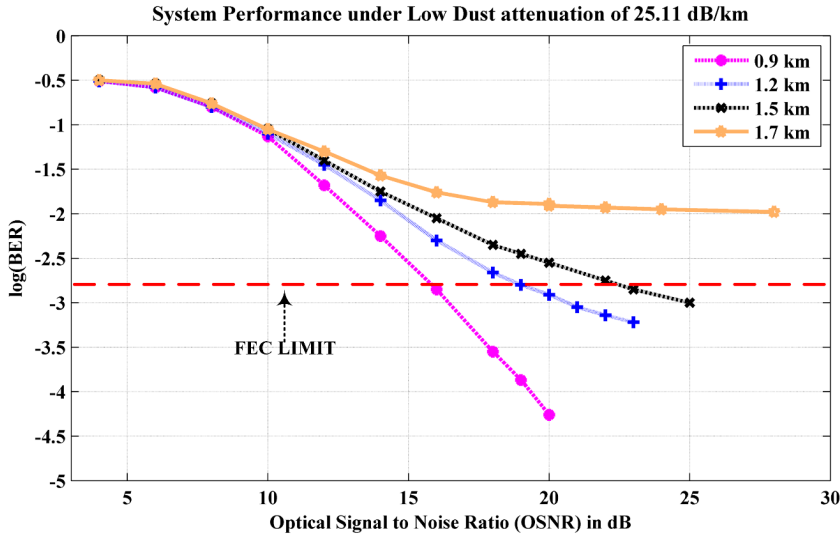


Fig. 7. BER vs. OSNR for different link range under LD condition.

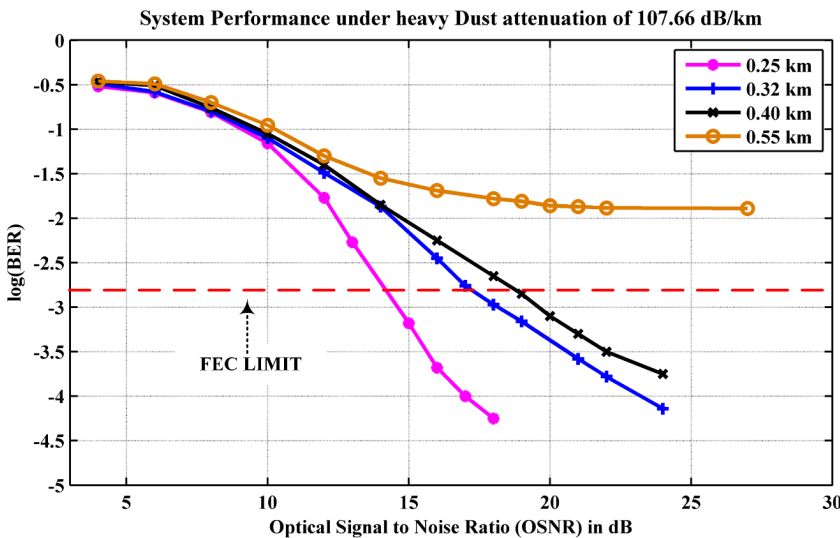


Fig. 8. BER vs. OSNR for different link range under MD condition.

observed that under low dust conditions, the maximum link range is achieved. The system operation cost can be minimized by optimizing the OSNR performance and maximizing the data transmission rate. Also, this OSNR tolerance level increases linearly and almost doubles with respect to data transmission rate [26].

Figures 7 and 8 illustrate the BER vs. OSNR performance comparison of the 120 Gb/s OAM polarized and 16 QAM modulated proposed homodyne FSO system for various transmission distances under different dust environments. The  $\log(\text{BER})$  values are decreasing exponentially with the increase in OSNR ranges from 4 to 30 dB. As shown in both the figures, to maintain the acceptable BER FEC limit less than  $2.2 \times 10^{-3}$ , the required OSNR is 21.9 dB for link distance of 1.5 km whereas it is 18.76 dB for link distance of 0.44 km under low and heavy dust scenario.

As illustrated in Fig. 9, the minimum link distances achieved for these OSNR under low and heavy dust conditions are 0.9 and 0.25 km, respectively, whereas the maximum link distance achieved for both the conditions are 1.5 and 0.40 km, respectively. The obtained result clearly demonstrates that under heavy dust condition, the system has the lowest propagation distance of 0.25 km due to the highest attenuation of 107.66 dB in the free space channel caused by the heavy dust.

The receiver sensitivity for the proposed system is demonstrated in Fig. 10, where the two dust scenarios are compared in terms of the received optical power at the receiver end. The simulation graph clearly shows the variation of  $\log(\text{BER})$  with respect to received optical power under two assumed dust weather conditions. As the received optical power increases from  $-40$  to  $-4$  dBm, the  $\log(\text{BER})$  performance also improves exponentially from  $-0.5$  to  $-4.4$  due to the least amount of error during the detection process. The receiver sensitivity archived for the proposed system is greater than

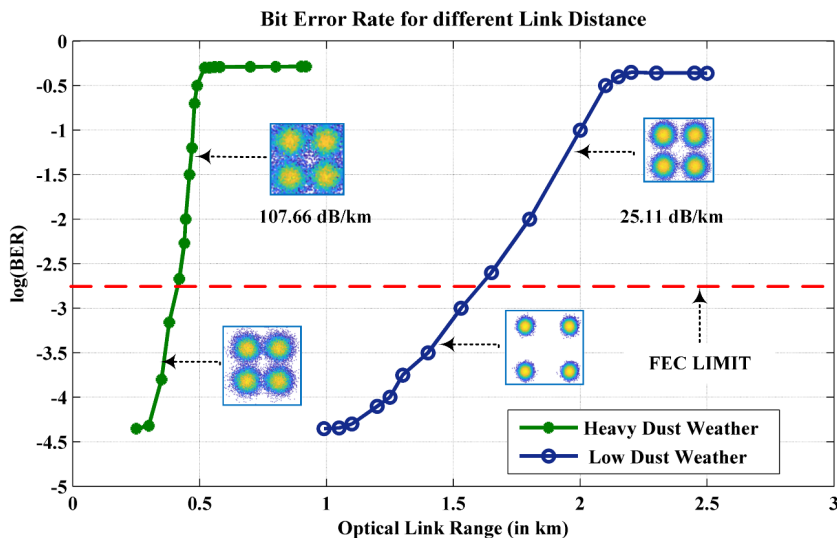


Fig. 9. BER vs. optical link range (in km) for low and heavy dust conditions.

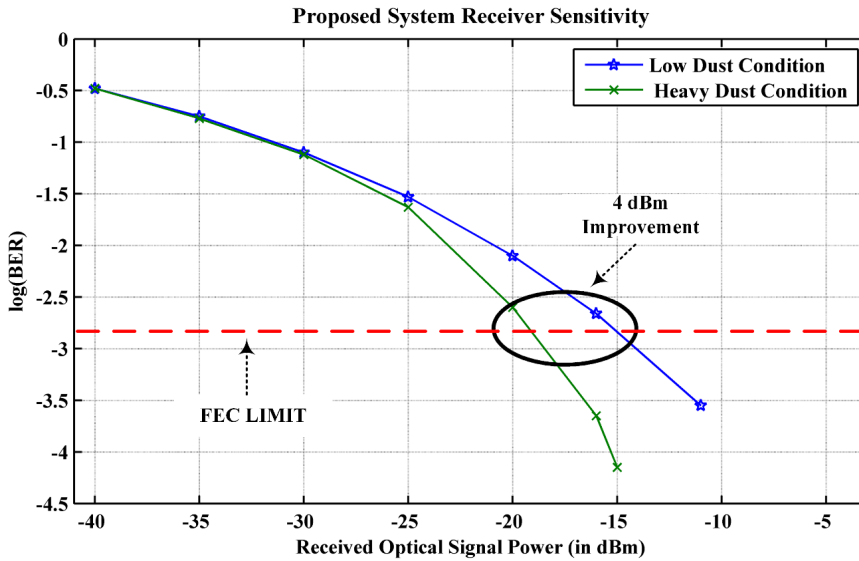


Fig. 10. BER vs. optical receiver sensitivity for the proposed system.

–17.8 dBm. For the BER FEC limit less than  $2 \times 10^{-3}$ , the received optical power in low dust conditions is –14.9 dBm, whereas under heavy dust, it is –18.3 dBm, which clearly demonstrates 4 dBm better performance by the proposed system under low dust environments compared to heavy dust. The system possesses a receiver sensitivity of –17.8 dBm.

Table 3 illustrates and compares the work implemented in this paper with the existing published work. The majority of the high-speed FSO system is tested in rain, fog, and haze. Very few researchers have focused on different desert weather condi-

T a b l e 3. Performance comparison of the proposed system with existing literature.

	Channel condition	Attenuation [dB/km]	Laser power [dBm]	Maximum data rate [Gb/s]	Range [km]
Hybrid PDM/OFDM [27]	Rain	15	10	5	3
	Fog	10			2.3
SAC-OCDMA-OAM [28]	Heavy rain	19.28	15	120	0.16
	Heavy haze	10.115			0.2
	Heavy fog	22			0.15
Hybrid SAC-OCDMA FSO-MDM [29]	Heavy haze	2.4	15	100	4
	Heavy rain	19.3			8
	Light fog	9			3.6
Hybrid OFDM-MDM [30]	Moderate fog	12	10	80	3
	Heavy fog	16			2
Present work	Light dust	25.11	15	120	1.5
	Heavy dust	107.66			0.4

tions. Although the attenuation level provided by desert conditions is nearly identical to that provided by fog weather performance, it is assumed to be higher for the proposed system. Taking this into account, our work outperforms the reference [28] in terms of link distances for the same transmission rate and higher attenuation levels. Comparably, our proposed system shows a higher data transmission rate for the higher side of weather attenuation levels.

## 6. Conclusion

In this work, we have presented and analyzed the OAM polarized 16 QAM-OFDM-MDM FSO coherent system under the low and heavy dust environment conditions. The system uses the two  $LG_{0,0}$  and  $LG_{0,10}$  QAM modes to carry the two independent 16-QAM and OFDM modulated data streams to enhance the system capacity. These streams are further multiplexed using MDM and transmitted over the different dust environments. At the receiver end, a DSP based coherent receiver structure is implemented to combat different signal impairments. The presented system supports a 120 Gb/s data rate at an acceptable optical SNR and maximum transmission ranges 1.5 km, and 0.40 km in low dust and heavy dust scenario, respectively. The system improvement can be further investigated for higher values of M-QAM modulation under other different conditions such as fog, haze, *etc.* Spatial diversity and channel coding techniques can be included in future. The proposed system can be a solution to support the next generation of high speed and high-capacity broadband services at a much-reduced cost.

## References

- [1] AL-GAILANI S.A., MOHD SALLEH M.F., SALEM A.A., SHADDAD R.Q., SHEIKH U.U., ALGEELENI N.A., ALMOHAMAD T.A., *A Survey of free space optics (FSO) communication systems, links, and networks*, IEEE Access **9**, 2021: 7353-7373. <https://doi.org/10.1109/ACCESS.2020.3048049>
- [2] KHALIGHI M.A., UYSAL M., *Survey on free space optical communication: A communication theory perspective*, IEEE Communications Surveys & Tutorials **16**(4), 2014: 2231-2258. <https://doi.org/10.1109/COMST.2014.2329501>
- [3] SINGH H., MITTAL N., MIGLANI R., SINGH H., GABA G.S., HEDABOU M., *Design and analysis of high-speed free space optical (FSO) communication system for supporting fifth generation (5G) data services in diverse geographical locations of India*, IEEE Photonics Journal **13**(5), 2021: 7300312. <https://doi.org/10.1109/JPHOT.2021.3113650>
- [4] MALIK A., SINGH P., *Free space optics: Current applications and future challenge*, International Journal of Optics, 2015: 945483. <https://doi.org/10.1155/2015/945483>
- [5] MATSUMOTO M., *Next generation free-space optical system by system design optimization and performance enhancement*, Progress in Electromagnetics Research Symposium, Kuala Lumpur, Malaysia, 2012: 501-506.
- [6] ALI M.A.A., AHMED E.H., *Performance of FSO communication system under various weather condition*, Advances in Physics Theories and Applications **43**, 2015: 10-18.
- [7] HASAN O., TAHA M., *Optimized FSO system performance over atmospheric turbulence channels with pointing error and weather conditions*, Radioengineering **25**(4), 2016: 658-665. <https://doi.org/10.13164/re.2016.0658>
- [8] ALI M.A.A., *Performance analysis of fog effect on free space optical communication system*, IOSR Journal of Applied Physics **7**(2), 2015: 16-24.

- [9] ZHANG J., LI Z., DANG A., *Performance of wireless optical communication systems under polarization effects over atmospheric turbulence*, Optics Communications **416**, 2018: 207-213. <https://doi.org/10.1016/j.optcom.2018.02.023>
- [10] MALLICK K., MANDAL P., MANDAL G.C., MUKHERJEE R., DAS B., PATRA A.S., *Hybrid MMW-over fiber/OFDM-FSO transmission system based on doublet lens scheme and POLMUX technique*, Optical Fiber Technology **52**, 2019: 101942. <https://doi.org/10.1016/j.yofte.2019.101942>
- [11] MUKHERJEE R., MALLICK K., KUIRI B., SANTRA S., DUTTA B., MANDAL P., PATRA A.S., *PAM-4 based long-range free-space-optics communication system with self-injection locked QD-LD and RS codec*, Optics Communications **476**, 2020: 126304. <https://doi.org/10.1016/j.optcom.2020.126304>
- [12] DUTTA B., KUIRI B., SANTRA S., SARKAR N., BISWAS I.A., ATTA R., PATRA A.S., *100 Gbps data transmission based on different l-valued OAM beam multiplexing employing WDM techniques and free space optics*, Optical and Quantum Electronics **53**, 2021: 515. <https://doi.org/10.1007/s11082-021-03154-w>
- [13] DUTTA B., SARKAR N., ATTA R., KUIRI B., SANTRA S., PATRA A.S., *640 Gbps FSO data transmission system based on orbital angular momentum beam multiplexing employing optical frequency comb*, Optical and Quantum Electronics **54**(2), 2022: 132. <https://doi.org/10.1007/s11082-021-03509-3>
- [14] ABD EL-MOTTALEB S.A., FAYED H.A., ABD EL-AZIZ A., METAWEE M.A., ALY M.H., *Enhanced spectral amplitude coding OCDMA system utilizing a single photodiode detection*, Applied Sciences **8**(10), 2018: 1861. <https://doi.org/10.3390/app8101861>
- [15] SARANGAL H., SINGH A., MALHOTRA J., CHAUDHARY S., *A cost effective 100 Gbps hybrid MDM- OCDMA -FSO transmission system under atmospheric turbulences*, Optical and Quantum Electronics **49**(5), 2017: 184. <https://doi.org/10.1007/s11082-017-1019-2>
- [16] SIVARANJANI M., VIDHYA J., *System performance of free space optics in underground moving train using opti system 14*, Asian Journal of Applied Science and Technology **1**(3), 2017: 232-235.
- [17] KUMAR A., SHARMA A., *A 5×16 Gbps DWDM system for ground-to-satellite using RZ signaling scheme under different turbulences*, Procedia Computer Science **115**, 2017: 115-122. <https://doi.org/10.1016/j.procs.2017.09.084>
- [18] RICHARDSON D.J., FINI J.M., NELSON L.E., *Space-division multiplexing in optical fibres*, Nature Photonics **7**(5), 2013: 354-362. <https://doi.org/10.1038/nphoton.2013.94>
- [19] YU Z.X., CAI R.J., WU Z.H., HE H.W., JIANG H.X., FENG X.L., ZHENG A.R., CHEN J.F., GAO S.M., *Performance evaluation of direct-detection coherent receiver array for free-space communications with full-link simulation*, Optics Communications **454**, 2020: 124520. <https://doi.org/10.1016/j.optcom.2019.124520>
- [20] PFAU T., HOFFMANN S., NOE R., *Hardware-efficient coherent digital receiver concept with feed-forward carrier recovery for M-QAM constellations*, Journal of Lightwave Technology **27**(8), 2009: 989-999. <https://doi.org/10.1109/JLT.2008.2010511>
- [21] CHAUDHARY S., TANG X., WEI X., *Comparison of Laguerre-Gaussian and Donut modes for MDM -WDM in OFDM-Ro-FSO transmission system*, AEU - International Journal of Electronics and Communications **93**, 2018: 208-214. <https://doi.org/10.1016/j.aeue.2018.06.024>
- [22] ESMAIL M.A., FATHALLAH H., ALOUINI M.-S., *Effect of dust storms on FSO communications links*, [In] *2016 4th International Conference on Control Engineering & Information Technology (CEIT)*, Hammamet, Tunisia, 2016: 1-6. <https://doi.org/10.1109/CEIT.2016.7929046>
- [23] KAUSHAL H., JAIN V.K., KAR S., *Free Space Optical Communication*, Springer, 2012.
- [24] BLOOM S., KOREVAAR E., SCHUSTER J., WILLEBRAND H., *Understanding the performance of free-space optics*, Journal of Optical Networking **2**(6), 2003: 178-200. <https://doi.org/10.1364/JON.2.000178>
- [25] ANDREWS L.C., PHILLIPS R.L., *Laser Beam Propagation through Random Media*, SPIE Press Book, 2005.
- [26] WINZER P.J., ESSIAMBRE R.-J., *Advanced optical modulation formats*, Proceedings of the IEEE **94**(5), 2006: 952-985. <https://doi.org/10.1109/JPROC.2006.873438>

- [27] KAUR G., SRIVASTAVA D., SINGH P., PARASHER Y., *Development of a novel hybrid PDM/OFDM technique for FSO system and its performance analysis*, Optics & Laser Technology **109**, 2019: 256-262. <https://doi.org/10.1016/j.optlastec.2018.08.008>
- [28] SINGH M., ATIEH A., ALY M.H., ABD EL-MOTTALEB S.A., *120 Gbps SAC-OCDMA-OAM-based FSO transmission system: Performance evaluation under different weather conditions*, Alexandria Engineering Journal **61**(12), 2022: 10407-10418. <https://doi.org/10.1016/j.aej.2022.03.070>
- [29] SARANGAL H., THAPAR S.S., NISAR K.S., SINGH M., MALHOTRA J., *Performance estimation of 100 GB/s hybrid SACOCDMA FSO-MDM system under atmospheric turbulences*, Optical and Quantum Electronics **53**(10), 2021: 598. <https://doi.org/10.1007/s11082-021-03257-4>
- [30] SINGH M., MALHOTRA J., *Long-reach high-capacity hybrid MDM-OFDM-FSO transmission link under the effect of atmospheric turbulence*, Wireless Personal Communications **107**, 2019: 1549-1571. <https://doi.org/10.1007/s11277-019-06345-7>

*Received November 21, 2022  
in revised form December 8, 2022*